Rate Constants of HO_2 + NO Covering Atmospheric Conditions. 1. HO_2 Formed by OH + H_2O_2

Birger Bohn and Cornelius Zetzsch*

Fraunhofer-Institut für Toxikologie und Aerosolforschung, Nikolai-Fuchs Strasse 1, D-30625 Hannover, Germany

Received: May 14, 1996; In Final Form: November 11, 1996[⊗]

Rate constants of the gas-phase reactions HO_2 + NO → products (1), HO_2 + NO → OH + NO_2 (1a), and OH + NO → products (2) were determined at room temperature and total pressures of 10, 50, and 100 kPa of N_2. OH radicals were produced by pulsed 248 nm photolysis of H_2O_2 and monitored by time-resolved CW UV-laser long-path absorption. Biexponential OH decay curves, observed in the presence of H_2O_2 and NO, were analyzed to obtain rate constants for the above reactions. Those of reactions 1 and 1a were found to be independent of pressure with averaged values of $(9.7 \pm 1.5) \times 10^{-12}$ and $(9.6 \pm 1.5) \times 10^{-12}$ cm^3 s^{-1}, respectively. This indicates an OH yield very close to unity ($\geq$0.95) for the title reaction under the experimental conditions of this work. Error limits are estimated considering statistical and possible systematic errors. The pressure dependence found for reaction 2 is in good agreement with literature data. Rate constants of $(1.3 \pm 0.4) \times 10^{-12}$, $(4.7 \pm 0.8) \times 10^{-12}$, and $(7.4 \pm 1.3) \times 10^{-12}$ cm^3 s^{-1} have been determined for total pressures of 10, 50, and 100 kPa of N_2, respectively. Addition of H_2O at mixing ratios of 1.7% had no influence on the investigated reactions. Moreover, a quantum yield $\leq$0.05 is estimated for the formation of H + HO_2 in the 248 nm photolysis of H_2O_2. The rate constants of the HO_2 + NO reaction are slightly larger (15%) than the most recent recommendations.

Introduction

The HO_2 radical is an important species in atmospheric and combustion chemistry. In the troposphere it mainly reacts with NO forming OH and NO_2.[1]

$$HO_2 + NO \rightarrow OH + NO_2 \qquad (1a)$$

The photolysis of NO_2 then leads to the formation of ozone.[1] The HO_2 + NO reaction has been investigated in a large number of studies before, and there is now good agreement on the rate constant at low pressure conditions.[2−11] On the other hand, studies of reaction 1 have not been performed at total pressures exceeding ≈2 kPa until recently.[11] The slightly negative temperature coefficient of the reaction[2−4,11] indicates the possibility of a transient complex formation[10,12] which might cause a pressure dependence of the rate constant (like, for example, in the HO_2 self-reaction[13]). Thus, a pressure-dependent study of the HO_2 + NO reaction covering the tropospheric pressure range was needed.

Two other reactions might compete with (1a) and have been discussed in the literature.[2,10]

$$HO_2 + NO \xrightarrow{M} HOONO \qquad (1b)$$

$$\rightarrow HNO + O_2 \qquad (1c)$$

Up to now, no indication for one of these reactions has been reported. The product of reaction 1b, peroxynitrous acid (HOONO), has been identified in argon matrices as a product of nitric acid photolysis[14] but could not be detected as a product of the OH + NO_2 reaction in the gas phase.[15] Alkyl peroxy radicals are known to react with NO forming an adduct with subsequent isomerization to the corresponding nitrates.[16] However, this process is only of importance for species containing more than three C atoms. Thus, although the energy released in the HO_2 + NO reaction is roughly a factor of 2 smaller,[17] a stabilization of HOONO, possibly followed by an isomerization into nitric acid, appears to be unlikely at atmospheric pressure conditions. Nevertheless, it could not be excluded totally and may be of importance at very high pressures.

In this work we have performed measurements at total pressures of 10, 50, and 100 kPa of N_2. The experimental method employed here allows us to determine the rate constants of reactions 1 and 1a, as well as that of the reaction of OH with NO, forming HONO.[18,19]

$$OH + NO \xrightarrow{M} HONO \qquad (2)$$

H_2O_2 is photolyzed in a 248 nm excimer laser pulse to produce ground state OH radicals. The reaction of OH with H_2O_2 forms HO_2

$$OH + H_2O_2 \rightarrow HO_2 + H_2O \qquad (3)$$

from which OH is regenerated in the presence of NO by reaction 1a. This results in biexponential OH decay curves that were analyzed to obtain the rate constants of the involved reactions.

Experimental Section

OH is monitored by time-resolved detection by CW UV-laser long-path absorption on the $Q_1(2)$ line of the OH(A←X) transition around 308 nm (path length 100 m, CW laser power ≈200 μW). This experimental method has been described before.[20−22] H_2O_2 concentrations varied between 1.5 and 4.5 Pa in a large excess of N_2. With the available excimer laser pulse energy (≈300 mJ in a beam diameter of 15 cm) this results in typical starting concentrations of about 5×10^{10} cm^{-3} of OH in a gas volume of approximately 20 L. This concentration is sufficient to obtain reasonable decay curves after averaging

[⊗] Abstract published in *Advance ACS Abstracts,* January 1, 1997.

S1089-5639(96)01396-5 CCC: $14.00

over 10−20 laser shots while it is small enough to ensure pseudo-first-order conditions.

The measurements were carried out at room temperature in slowly flowing gas mixtures at total pressures of 10, 50, and 100 kPa of N_2 containing 5, 0.4, and 0.1% of O_2, respectively. O_2 was added in order to convert H atoms, possibly formed in the H_2O_2 photolysis, into HO_2. The gases had minimum purities of 99.999% (N_2), 99.995% (O_2), and 99.5% (NO) stated by the manufacturer (Messer Griesheim). The combination of mass-flow controllers (FC 260, Tylan) with capacitance manometers (Baratron, MKS) allows us to adjust concentrations and total pressure. NO pressures were varied between 0.2 and 0.6 Pa. Diluted gas mixtures containing 300 or 2000 ppm of NO in N_2 or Ar were used. The concentrations have stated uncertainties of 2% (Messer Griesheim). Before entering the cell these mixtures were fed through a glass tube filled with solid iron(II) sulfate ($FeSO_4 \cdot 5H_2O$) in order to remove NO_2 traces.

Measurements at a given total pressure were made with at least two significantly different H_2O_2 concentrations in the range given above. The dosage of H_2O_2 by purging a concentrated liquid solution with inert gas, as well as its limited stability in the reaction cell have been discussed in our recent work on the OH + C_2H_2 reaction.[22] H_2O_2 concentrations were calculated by measuring the OH decay rate in the absence of other reactants (τ_0^{-1}), using a rate constant of 1.75×10^{-12} cm^3 s^{-1} for the OH + H_2O_2 reaction.[23] No evidence for significant OH losses due to background impurities was found. A plot of the gas flow purging the H_2O_2 solution against τ_0^{-1} gave a linear dependence leading through the origin in good approximation. We estimate that the OH loss rate coefficient in the absence of H_2O_2 is below 10 s^{-1} for the total pressures used here.

Since NO losses are recognized in the OH time behavior even after only 10 laser shots, the reaction cycle initiated by the production of OH appears to be very effective. As a consequence, decay curves were recorded by averaging over three laser shots for the time being. Due to the large volume (≈20 L) and the limited total gas flow (≈3 L/min (STP)) 20 min were then allowed to elapse until the next measurement was started. This procedure was repeated about 10 times to complete a measurement.

Figure 1 shows typical decay curves obtained with different NO concentrations. The recorded signal is an amplified transient difference in photocurrents, proportional to the absorptance of the gas mixture and thus to the OH concentration at low optical densities. At $t \leq 0.1$ ms an increase of the signal can be recognized owing to the rise time of the amplifier acting as a low-pass filter. As a consequence, the absorption signals are recorded somewhat delayed with respect to their real time behavior. To describe the time dependence of the recorded signal the convolution integral of the filter function, with time constant τ_D, and the time dependence of the OH concentration has to be calculated. In case of a biexponential OH time dependence

$$[\mathrm{OH}](t)/[\mathrm{OH}]_{t=0} = c_1 \exp(-t/\tau_1) + c_2 \exp(-t/\tau_2) \quad (4)$$

which will be discussed in more detail below, the convolution integral results in the following expression for the recorded signal.

$$\Delta I_{\mathrm{rec}}(t) \propto \frac{c_1}{1-\tau_D/\tau_1}\exp(-t/\tau_1) + \frac{c_2}{1-\tau_D/\tau_2}\exp(-t/\tau_2) - \left(\frac{c_1}{1-\tau_D/\tau_1} + \frac{c_2}{1-\tau_D/\tau_2}\right)\exp(-t/\tau_D) \quad (5)$$

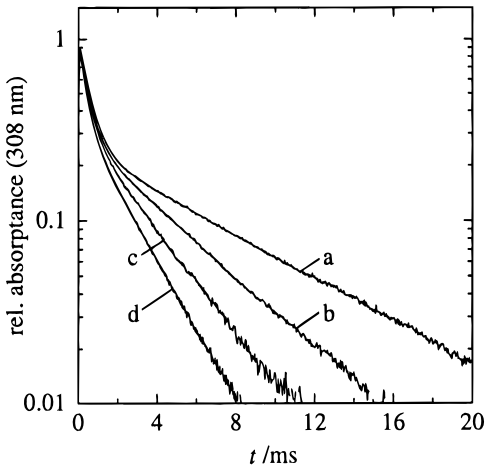

Figure 1. Typical biexponential OH decay curves in a semilogarithmic plot obtained at a total pressure of 100 kPa of N_2, an H_2O_2 concentration of 5.6×10^{14} cm^{-3} and different NO levels. [NO]/10^{14} cm^{-3}: (a) 0.60, (b) 0.85, (c) 1.09, and (d) 1.34. The displayed curves are averaged over 30 single measurements (30 laser shots) and normalized to the same extrapolated amplitudes at $t = 0$. At very short times (≤0.1 ms) a rise of the absorption signal can be recognized, caused by the time constant of the detection system.

The time constant τ_D has been determined to be 25 ± 5 μs in a nonlinear least squares fit to decay curves using the highest possible time resolution (10 μs) and carefully avoiding stray light from the excimer laser. For $t \geq 0.2$ ms the last term of eq 5 vanishes, and a biexponential time dependence with the same time constants as in eq 4 remains. Thus, the experimentally recorded decay curves were analyzed for $t \geq 0.2$ ms and referred to as biexponential in a nonlinear least-squares fit with amplitudes that were corrected according to eq 5, i.e., multiplied by $(1 - \tau_D/\tau_i)$. In the fitting procedure five parameters have been considered: the amplitudes and time constants of the two exponentials (eq 4), and the background signal. Corrections of the amplitude of the exponential with the smaller time constant (usually referred to as 1) are in the range of 4−8%.

Results

Evaluation of Rate Constants. The following scheme shows the reactions occurring in the presence of NO and H_2O_2 after an initial production of OH (or HO_2).

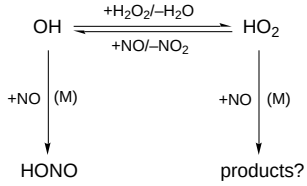

The corresponding system of differential equations for the radical concentrations

$$\mathrm{d}[\mathrm{OH}]/\mathrm{d}t = -{}^1k_{\mathrm{l,OH}}[\mathrm{OH}] + {}^1k_{\mathrm{f,OH}}[\mathrm{HO_2}] \quad (6)$$

$$\mathrm{d}[\mathrm{HO_2}]/\mathrm{d}t = {}^1k_{\mathrm{f,HO_2}}[\mathrm{OH}] - {}^1k_{\mathrm{l,HO_2}}[\mathrm{HO_2}] \quad (7)$$

which can be solved analytically[24] results in a biexponential time dependence for the OH concentration according to eq 4.

The time constants τ_1 and τ_2 depend on the formation ($^1k_{\mathrm{f}}$) (the index 1 at the ^1k values indicates pseudo-first-order rate constants) and loss ($^1k_{\mathrm{l}}$) rate coefficients of OH and HO_2, while the amplitudes c_1 and c_2 also depend on starting conditions. In the special case that only OH is present at $t = 0$, which will be

shown to be the case here, the following relationships can be derived.

$$ {}^1k_{l,HO_2} = \frac{\tau_1^{-1} + c_1/c_2 \cdot \tau_2^{-1}}{c_1/c_2 + 1} \quad (8) $$

$$ {}^1k_{l,OH} = \tau_1^{-1} + \tau_2^{-1} - {}^1k_{l,HO_2} \quad (9) $$

$$ {}^1k_{f,OH}\,{}^1k_{f,HO_2} = {}^1k_{l,HO_2}\,{}^1k_{l,OH} - \tau_1^{-1}\tau_2^{-1} \quad (10) $$

The amplitudes c_1 and c_2 appear as a ratio. By this the proportionality factor in eq 5, containing the initial OH concentration, cancels out. On the other hand, OH and HO_2 formation rate coefficients only occur as a product. Fortunately, in the present system the HO_2 formation rate coefficient can be determined independently by measuring the OH loss rate coefficient in the absence of NO (τ_0^{-1}). In case that (i) the loss of OH is only due to reaction with H_2O_2, as confirmed in the Experimental Section, and (ii) assuming an HO_2 yield of unity for the H_2O_2 + OH reaction (3),[25] the HO_2 formation rate coefficient is given by

$$ {}^1k_{f,HO_2} = k_3[H_2O_2] = \tau_0^{-1} \quad (11) $$

Thus, the OH formation rate coefficient ${}^1k_{f,OH}$ can be calculated from eqs 8−10.

$$ {}^1k_{f,OH} = ({}^1k_{l,HO_2}\,{}^1k_{l,OH} - \tau_1^{-1}\tau_2^{-1})\tau_0 \quad (12) $$

Table 1 summarizes the biexponential curve parameters, obtained for different NO concentrations and the independently measured values of τ_0^{-1}.

HO_2 + NO Reaction. Figure 2 shows HO_2 loss and OH formation rate coefficients as a function of NO concentration. Different H_2O_2 pressures do not influence these coefficients, as expected from the reaction model. Within the scatter of the data there is neither a pressure dependence nor a difference in OH formation and HO_2 loss rate coefficients noticeable. This is confirmed in Table 2 showing the results from linear regressions of the data to obtain the rate constants k_1 and k_{1a} for the different total pressures according to the following equations.

$$ {}^1k_{l,HO_2} = k_1[NO] + c_{l,HO_2} \quad (13) $$

$$ {}^1k_{f,OH} = k_{1a}[NO] + c_{f,OH} \quad (14) $$

No indication for an HO_2 loss or OH formation not due to the reaction with NO was found. The fitted intercepts c_{l,HO_2} and $c_{f,OH}$ for the coefficients were found to be slightly negative ($\approx -(30 \pm 40)s^{-1}$), but zero within their 2σ error limits. This may be taken as a hint at a small loss of NO caused by the effective chain reaction, even while proceeding with very few laser shots, as described in the Experimental Section. However, the influence of this possible loss is smaller than the 2σ error limits stated in Table 2.

The OH yields of the HO_2 + NO reaction, i.e. the fractions of the rate constants k_{1a} and k_1, are also given in Table 2. They were obtained by linear regressions from plots of the rate coefficients from eqs 13 and 14 against each other. The OH yields are unity in all cases with 2σ errors limits ≤5%.

Filled circles in Figure 2 indicate measurements made in the presence of water vapor with a mixing ratio of 0.017. Since no effect was observed, no further measurements were performed in the presence of water.

TABLE 1: NO Concentrations, Fitted Decay Curve Parameters, τ_1^{-1}, τ_2^{-1}, and c_1/c_2 (Corrected According to Eq 5), and OH Decay Rates, τ_0^{-1} (Measured in the Absence of NO)

$[NO]/10^{14}$ cm^{-3}	$\tau_1^{-1}/10^3$ s^{-1}	$\tau_2^{-1}/10^2$ s^{-1}	c_1/c_2	$\tau_0^{-1}/10^3$ s^{-1}
		$p = 9.9$ kPa		
0.55	1.56	0.30	2.23	1.01
0.62	1.67	0.35	2.05	1.03
0.73	1.34	0.52	1.05	0.61
0.74	1.72	0.45	1.65	1.00
0.90	1.95	0.57	1.44	1.03
1.02	2.02	0.68	1.24	1.00
1.12	1.69	0.93	0.69	0.61
1.17	2.20	0.86	1.08	1.02
1.28	2.31	0.97	0.97	1.01
1.42	2.42	1.13	0.86	0.99
0.70[a]	1.41	0.49	1.23	0.71
1.03[a]	1.74	0.89	0.82	0.71
		$p = 50.0$ kPa		
0.35	1.14	0.46	3.16	0.74
0.56	1.81	0.77	3.00	1.15
0.57	1.68	0.82	2.73	1.01
0.59	1.44	1.06	2.02	0.73
0.78	1.64	1.56	1.64	0.74
0.81	2.25	1.28	2.30	1.27
0.87	2.45	1.28	2.61	1.45
1.00	2.32	1.87	1.89	1.15
1.05	2.31	2.11	1.65	1.08
1.20	2.89	2.14	2.00	1.44
1.27	2.78	2.52	1.71	1.29
1.40	2.97	2.85	1.63	1.30
0.52[a]	1.83	0.64	3.30	1.21
0.85[a]	2.24	1.69	2.32	1.21
		$p = 99.8$ kPa		
0.59	2.70	0.94	5.08	1.89
0.60	1.83	1.36	3.02	0.99
0.71	2.46	1.28	3.54	1.44
0.77	2.99	1.38	4.13	1.88
0.85	2.17	2.23	2.45	0.99
0.96	2.83	2.11	2.90	1.47
1.08	3.39	2.40	3.08	1.87
1.09	2.42	3.27	2.07	0.98
1.21	3.25	3.32	2.56	1.53
1.30	3.71	3.10	2.74	1.87
1.34	2.79	4.39	1.84	0.98
1.14[a]	3.00	3.01	2.57	1.40
1.41[a]	3.37	4.10	2.24	1.41

[a] Measurements in the presence of 1.7% of water vapor, not considered in the evaluation of the rate constants in Table 2.

OH + NO Reaction. As expected from the reaction model, the OH loss rate coefficient was found to depend on total pressure and NO and H_2O_2 concentration.

$$ {}^1k_{l,OH} = k_2[NO] + k_3[H_2O_2] + c_{l,OH} \quad (15) $$

In order to determine the rate constant k_2, measurements with different H_2O_2 concentrations were combined by subtracting the τ_0^{-1} values measured in the absence of NO (eq 11). The result is shown in Figure 3 for the different total pressures used here. The straight lines correspond to the rate constants given in Table 2. The intercepts $c_{l,OH}$ were found to be zero in good approximation ($\approx -(10 \pm 40)s^{-1}$). This is not in contradiction to the suggestion that a loss of NO is responsible for the slightly negative intercepts found for the HO_2 loss rate coefficients: NO_2 is formed when NO and H_2O_2 are consumed and NO_2 is reactive with respect to OH. However, the amount of NO_2 formed this way is not expected to have a significant influence on the present reaction system.

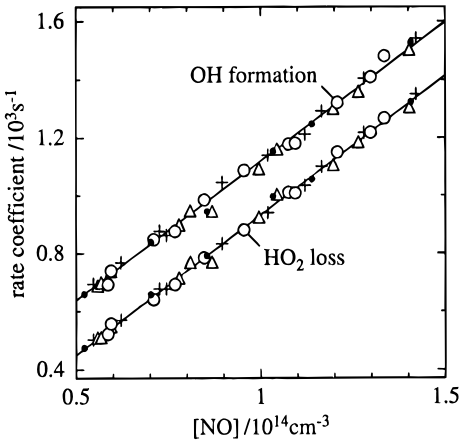

Figure 2. OH formation rate coefficient ($^1k_{f,OH}$) and HO_2 loss rate coefficient ($^1k_{l,HO_2}$) dependences on the NO concentration for total pressures of approximately 100 (○), 50 (△), and 10 (×) kPa total pressure of N_2. The straight lines indicate averaged rate constants from Table 2. OH formation rate coefficients are shifted by 200 s^{-1} for clarity. Filled circles indicate measurements at water vapor mixing ratios of 0.017 at different total pressures (to assign total pressures refer to Figure 3 or Table 1).

TABLE 2: Rate Constants[a] (k_1, k_{1a}) and OH Yield[b] (ϕ_{OH}) of the Reaction HO_2 + NO, and Rate Constant[a] of the Reaction OH + NO (k_2) for Different Total Pressures of N_2, T = 297 ± 2 K

$p(N_2)$/kPa	k_1	k_{1a}	ϕ_{OH}	k_2
9.9	9.7 ± 0.3	9.6 ± 0.4	0.99 ± 0.03	1.3 ± 0.3
50.0	9.5 ± 0.4	9.5 ± 0.3	1.00 ± 0.03	4.7 ± 0.3
99.8	9.8 ± 0.4	9.7 ± 0.6	1.00 ± 0.05	7.4 ± 0.6

[a] Error limits are 2σ (statistical). Units are 10^{-12} cm^3 s^{-1}, an additional relative error of 10% is estimated from uncertainties of gas-flow rates, pressure determination and further possible systematic errors. [b] Slopes taken from a correlation of the rate coefficients in Figure 2.

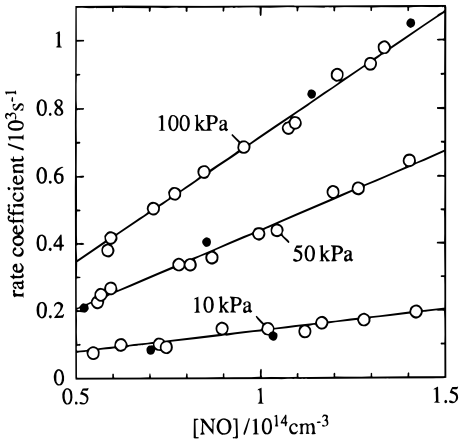

Figure 3. OH loss rate coefficients ($^1k_{l,OH}$) as a function of NO concentration for different total pressures of N_2. The data are normalized to $[H_2O_2] = 0$ by subtracting the OH loss rate coefficient in the absence of NO, measured in any case before and after addition of NO. The straight lines indicate the rate constants k_2 in Table 2. Filled circles indicate measurements at water vapor mixing ratios of 0.017.

The measured k_2 values are in good agreement with recent literature data.[19,26]

H + HO_2 Formation in H_2O_2 Photolysis. Recently, a quantum yield for OH formation significantly below 2 (ϕ_{OH} = 1.58 ± 0.23) has been reported by Schiffman et al.[23] for the 248 nm photolysis of H_2O_2. If H + HO_2 are photolysis products formed together with OH they are expected to influence the present system. Although a significant formation of H atoms has already been excluded in the literature,[27,28] we will show that also the data of this work are inconsistent with this possibility. As mentioned in the Experimental Section, small amounts of O_2 were added to provide a rapid conversion of possibly formed H atoms into HO_2 (τ(H)≈30−60 μs).[26] Considering the different starting conditions, eq 8 has to be modified.

$$^1k_{l,HO_2} = \frac{1}{2f} + \frac{(\tau_1^{-1} + \tau_2^{-1})}{2} - \left[\frac{\{f(\tau_1^{-1} - \tau_2^{-1}) + 1\}^2}{4f^2} - \frac{(\tau_1^{-1} - \tau_2^{-1})}{f(c_1/c_2 + 1)}\right]^{1/2} \quad (16)$$

The quantity f depends on the ratio of (H + HO_2) and OH formed in the photolysis and the independently measured value of τ_0, which again is taken as the reciprocal of the HO_2 formation rate coefficient.

$$f = \frac{[H + HO_2]_{t=0}}{[OH]_{t=0}} \tau_0 \quad (17)$$

Of course, in the limit $f \rightarrow 0$, eq 16 corresponds to eq 8.

All decay curves were analyzed a second time by taking the ratio $[H + HO_2]_{t=0}/[OH]_{t=0}$ = 0.25 which is the expected maximum value, corresponding to an OH quantum yield of 1.6.[23] Virtually no difference in the quality of the fits was found. The NO dependences of the different coefficients were linear as in Figures 2 and 3. However, the slopes and thus the rate constants were different. The measurements at a total pressure of 100 kPa gave no indication on which attempt is correct. Rate constants ($\pm 2\sigma$) $k_1 = (7.8 \pm 0.4) \times 10^{-12}$ cm^3 s^{-1}, $k_{1a} = (7.9 \pm 0.5) \times 10^{-12}$ cm^3 s^{-1}, and $k_2 = (9.0 \pm 0.8) \times 10^{-12}$ cm^3 s^{-1} were derived, which are in reasonable agreement with literature data.[17,26]

On the other hand, the results at lower total pressures are increasingly inconsistent. At 10 kPa k_2 would be a factor of 2.5 higher than recent literature values.[19,26] Furthermore, k_1 and k_{1a} would exhibit slight pressure dependences with different directions. Between 10 and 100 kPa k_1 would increase by 12% and k_{1a} decrease by 20%. Thus, with decreasing pressure the OH yield of reaction 1 would increase to physically meaningless values (up to ≈1.4 at 10 kPa). From these results we estimate an upper limit of 0.05 for the quantum yield of H + HO_2 formation in the 248 nm photolysis of H_2O_2 in accordance with literature.[27,28]

Discussion

In 1977 Howard[29] realized that the rate constants of the HO_2 + NO reaction measured before were too small. This was verified by Howard and Evenson[2] and other authors.[3−11] Table 3 summarizes room temperature measurements on the rate constant that have been made in the meantime. All data agree within the stated uncertainties except those of Thrush and Wilkinson[8] and Rozenshtein et al.[9] due to their relatively small error limits (1σ, not considering possible systematic errors). Up to now, all experiments have been performed in flow tubes, in most cases with LMR detection of HO_2. This technique is limited to total pressures below ≈2 kPa for reasons of pressure broadening. Very recently, Seeley et al.[11] have performed measurements at total pressures of up to 25 kPa using a turbulent flow technique and chemical ionization mass spectroscopy detection. These authors[11] found no pressure dependence of the rate constant in agreement with the results reported here. The data of the present study are the first measurements at

TABLE 3: Literature Data on the Rate Constant of the HO_2 + NO Reaction at Room Temperature

references	$k_1/10^{-12}$ cm^3 s^{-1}
Howard and Evenson (1977)[2]	$8.1 \pm 1.5^{a,b}$
Howard (1979)[3]	$8.0 \pm 1.0^{a,b}$
Leu (1979)[4]	$9.8 \pm 1.6^{a,b}$
Burrows et al. (1979)[5]	8.2 ± 2.4
Glaschick-Schimpf et al. (1979)[6]	11 ± 3^{b}
Hack et al. (1980)[7]	$7.6 \pm 1.7^{a,b}$
Thrush and Wilkinson (1981)[8]	$6.9 \pm 0.6^{a,b}$
Rozenshtein et al. (1984)[9]	7.0 ± 0.6
Jemi-Alade and Thrush (1990)[10]	$8.5 \pm 1.3^{a,b}$
Seeley et al. (1996)[11]	8.0 ± 1.2
recommendations	
IUPAC (1992)[26]	$8.3 \pm {}^{2.2}_{1.7}$
NASA (1994)[17]	$8.6 \pm {}^{1.7}_{1.4}$
this work	9.7 ± 1.5^{c}

[a] Considered in IUPAC recommendation. [b] Considered in NASA recommendation. [c] Error limit estimated considering statistical (Table 2) and possible systematic errors (10%).

pressures of up to 100 kPa covering the entire tropospheric pressure range.

The current IUPAC[26] and NASA[17] recommendations are also given in Table 3. They more or less represent averages of the given literature values, not including the most recent data by Seeley et al.[11] The averaged rate constant determined in the present work agrees within the error limits of the recommendations but our value is about 15% higher. This is expected to have a considerable influence on atmospheric chemistry models. In view of the more or less indirect procedure of deriving the rate constants adopted here, we will demonstrate that this difference cannot be explained by systematic deviations introduced in the data analysis.

For this purpose a nonlinear least-squares fit was performed with two of the decay curves from Figure 1 in which the rate parameters from eqs 8−10 are determined directly together with the total amplitude and the background signal (again omitting data points for $t \leq 0.2$ ms and after correction according to eq 5. From these parameters, which were found to be identical to those obtained using the alternative procedure, the corresponding model curves were constructed and subtracted from the corrected experimental curves. The residuals, normalized to a total amplitude of the decay curves of unity as in Figure 1, are displayed in Figure 4. The deviations are of the order of 0.2%, independent of time. Then the fit was repeated with the parameters ${}^1k_{l,HO_2}$ and ${}^1k_{f,OH}{}^1k_{f,HO_2}$ multiplied by a factor of 0.88 (the ratio 8.5/9.7 of the rate constants under consideration) and held fixed, while ${}^1k_{l,OH}$ (i.e., k_2), the total amplitude and the background were adjusted. Note that an OH yield of unity for the HO_2 + NO reaction is assumed in this procedure. The fitted OH loss rate coefficients showed only a small variation, resulting in changes in k_2 of −4% and −1.2% for curves (a) and (d), respectively. However, although the fitted decay curves appear quite similar to those obtained before at first glance, the curve parameters were found to have changed significantly by −4% and −5% (τ_1^{-1}), −12% and −9% (τ_2^{-1}), and +14% and +19% (c_1/c_2) for curves (a) and (d), respectively. Moreover, the quality of the fits decreased markedly, increasing χ^2 values by factors of 9.5 (a) and 8.3 (d). This is also reflected in the corresponding residuals displayed in Figure 4. It was checked that these deviations can not be attributed to the initial procedure of correcting the amplitudes.

Fixing only the value of ${}^1k_{l,HO_2}$ (i.e., k_1 to 8.5×10^{-12} cm^3 s^{-1}) resulted in a stronger change in k_2 of −30% and −18% for curves (a) and (d), respectively, while the OH yield of the HO_2 + NO reaction dropped to 87% in both cases. However,

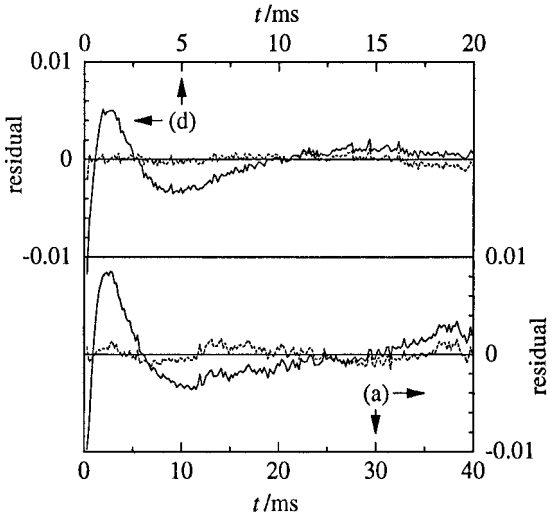

Figure 4. Residuals of nonlinear least square fits to decay curves (a) and (d) from Figure 1. Dotted line: result of a five-parameter fit including the total amplitude, the reaction rate parameters from eqs. 8−10 and the background signal. Full line: result of the same fit with the two parameters concerning the HO_2 + NO reaction scaled by a factor of 0.88 and held fixed (see text). Five-point averages of the data originally recorded are displayed.

the χ^2 values remain higher by factors of 5.4 (a) and 3.5 (d) than in the original fit.

From these results it is evident that the experimentally obtained curves are inconsistent with a rate constant significantly below 9.7×10^{-12} cm^3 s^{-1} for the HO_2 + NO reaction. The reproducibility of this result is reflected in the scatter of the data in Figures 2 and 3 and in the statistical errors of the linear regressions given in Table 2. Moreover, the independence of the rate parameters concerning the HO_2 reaction on the H_2O_2 concentration supports the validity of the kinetic model employed. NO concentrations are estimated to be precise within 5%. Two different gas mixtures were used in combination with two different flow controllers without any noticeable effect. However, considering the suspected NO losses due to the chain reaction, background signal fluctuations, the stated error of the amplifier time constant, and uncertainties in the determination and constancy of τ_0^{-1}, we estimate a relative error of 10% in addition to the statistical error limits stated in Table 2. The quantum yield of OH formation in the 248 nm photolysis of H_2O_2 has not been considered here as a possible error source, as will be discussed below. At last our result is confirmed independently in the second part of the paper,[30] where a different experimental technique is applied and the rate constant has also been studied temperature dependent.

The OH yield of unity found for the HO_2 + NO reaction shows that neither channel 1b or 1c nor an isomerization of a possible HOONO intermediate to HNO_3 is of importance under the experimental conditions of this work. Since no deviation from a biexponential OH decay behavior has been observed, HOONO is either not formed or it dissociates to OH + NO_2 within less than ≈1 ms. The latter is possible in view of a recently calculated dissociation energy of only 66 kJ mol^{-1} for the O−O bond in HOONO.[31] However, since no indication for a pressure dependence of the rate constant was found, a complex mechanism for the reaction appears to be unlikely. The OH yields of the reaction were determined from correlations of the rate coefficients in Figure 2. They are therefore widely unaffected by the possible errors discussed for the rate constants, for example by the uncertainties in NO concentrations. Thus, a lower limit of 95% for the OH yield is derived from the stated statistical errors in Table 2.

The rate constant of the HO_2 self-reaction has been shown to depend on the presence of water vapor.[13] This effect has been attributed to a complex formation followed by a displacement reaction.[32] An HO_2-H_2O complex may also exhibit different reactive properties with respect to NO. However, under our experimental conditions we did not observe a significant effect of water vapor on the HO_2 loss rate coefficient. At the highest total pressure of 100 kPa, the water vapor mixing ratio of 0.017 used here corresponds to a partial pressure of 1.7 kPa, which is roughly half of the vapor pressure at room temperature (i.e., 50% relative humidity). The enhancement of the $HO_2 + HO_2$ reaction is about a factor of 2 under these conditions.[13] We therefore conclude that the presence of water vapor has no influence on the HO_2 + NO reaction in the atmosphere.

The thorough work by Schiffman et al.[23] on the OH quantum yields of the 193 and 248 nm photolyses of H_2O_2 and HNO_3 has been carried out considering a large number of experimental parameters. Moreover, the vibrational Einstein transition probability used to calculate OH radical concentrations has been stated to be precise within 10%.[23] However, the reason for the measured low OH quantum yield[23] in the 248 nm photolysis remains unknown. The data obtained here confirm the more precise results on H-atom formation by Stief and DeCarlo[27] ($\phi_H + \phi_{HO_2} \leq 0.02$) and Vaghjiani and Ravishankara[28] ($\phi_H \leq 0.0001$). Energetically, formation of $O(^1D)$ or $O(^3P) + H_2O$ and $H_2 + O_2$ is also possible.[23] However, these products are not expected to influence the present reaction system and their formation has been excluded experimentally.[27,28]

Acknowledgment. Financial support by the Bundesminister für Bildung, Forschung und Technologie (grant FKZ 07 EU 705A/0) and the Commission of the European Communities (grant EV5V-CT93-0309) is gratefully acknowledged.

References and Notes

(1) Wayne, R. P. *Chemistry of Atmospheres*; Clarendon Press, Oxford, U.K., 1985.
(2) Howard, C. J.; Evenson, K. M. *Geophys. Res. Lett.* **1977**, *4*, 437.
(3) Howard, C. J. *J. Chem. Phys.* **1979**, *71*, 2352.
(4) Leu, M.-T. *J. Chem. Phys.* **1979**, *70*, 1662.
(5) Burrows, J. P.; Cliff, D. I.; Harris, G. W.; Thrush, B. A.; Wilkinson, J. P. T. *Proc. R. Soc. London A* **1979**, *368*, 463.
(6) Glaschick-Schimpf, I.; Leiss, A.; Monkhouse, P. B.; Schurath, U.; Becker, K. H.; Fink, E. H. *Chem. Phys. Lett.* **1979**, *67*, 318.
(7) Hack, W.; Preuss, A. W.; Temps, F.; Wagner, H. Gg.; Hoyermann, K. *Int. J. Chem. Kinet.* **1980**, *12*, 851.
(8) Thrush, B. A.; Wilkinson, J. P. T. *Chem. Phys. Lett.* **1981**, *81*, 1.
(9) Rozenshtein, V. B.; Gershenzon, Yu. M.; Il'In, S. D.; Kishkovitch, O. P. *Chem. Phys. Lett.* **1984**, *112*, 473.
(10) Jemi-Alade, A. A.; Thrush, B. A. *J. Chem. Soc., Faraday Trans.* **1990**, *86*, 3355.
(11) Seeley, J. V.; Meads, R. F.; Elrod, M. J.; Molina, M. J. *J. Phys. Chem.* **1996**, *100*, 4026.
(12) Troe, J. *J. Chem. Soc., Faraday Trans.* **1994**, *90*, 2303.
(13) Kircher, C. C.; Sander, S. P. *J. Phys. Chem.* **1984**, *88*, 2082.
(14) Cheng, B.-M.; Lee, J.-W.; Lee, Y.-P. *J. Phys. Chem.* **1991**, *95*, 2814.
(15) Burkholder, J. B.; Hammer, P. D.; Howard, C. J. *J. Phys. Chem.* **1987**, *91*, 2136.
(16) Atkinson, R.; Carter, W. P. L.; Winer, A. M. *J. Phys. Chem.* **1983**, *87*, 2012.
(17) DeMore, W. B.; Sander, S. P.; Golden, D. M.; Hampson, R. F.; Kurylo, M. J.; Howard, C. J.; Ravishankara, A. R.; Kolb, C. E.; Molina, M. J. *Chemical Kinetics and Photochemical Data for Use in Stratospheric Modeling, Evaluation Number 11*; JPL Publication 94−26, Jet Propulsion Laboratory, Pasadena, CA, 1994.
(18) Stuhl, F.; Niki, H. *J. Chem. Phys.* **1972**, *57*, 3377.
(19) Forster, R.; Frost, M.; Fulle, D.; Hamann, H. F.; Hippler, H.; Schlepegrell, A.; Troe, J. *J. Chem. Phys.* **1995**, *103*, 2949.
(20) Wahner, A. Ph.D. Thesis, Ruhr-Universität Bochum, Bochum, Germany, 1984.
(21) Wahner, A.; Zetzsch, C. *Ber. Bunsenges. Phys. Chem.* **1985**, *89*, 323.
(22) Bohn, B.; Siese, M.; Zetzsch, C. *J. Chem. Soc., Faraday Trans.* **1996**, *92*, 1459.
(23) Schiffman, A.; Nelson, D. D., Jr.; Nesbitt, D. J. *J. Chem. Phys.* **1993**, *98*, 6935.
(24) Wahner, A.; Zetzsch, C. *J. Phys. Chem.* **1983**, *87*, 4945.
(25) Vaghjiani, G. L.; Ravishankara, A. R.; Cohen, N. *J. Phys. Chem.* **1989**, *93*, 7833.
(26) Atkinson, R.; Baulch, D. L.; Cox, R. A.; Hampson, R. F., Jr.; Kerr, J. A.; Troe, J. *J. Phys. Chem. Ref. Data* **1992**, *21*, 1187.
(27) Stief, L. J.; DeCarlo, V. J. *J. Chem. Phys.* **1969**, *50*, 1234.
(28) Vaghjiani, G. L.; Ravishankara, A. R. *J. Chem. Phys.* **1990**, *92*, 996.
(29) Howard, C. J. *J. Chem. Phys.* **1977**, *67*, 5258.
(30) Koch, R. *J. Phys. Chem.*, submitted for publication.
(31) McGrath, M. P.; Francl, M. M.; Rowland, F. S.; Hehre, W. J. *J. Phys. Chem.* **1988**, *92*, 5352.
(32) Mozurkewich, M.; Benson, S. W. *Int. J. Chem. Kinet.* **1985**, *17*, 787.